



Cement-Based Composites Incorporating Pseudoboehmite Nanomaterials

Caroline Valadão Pacheco¹; Renato Meneghetti Peres²; Gabriela Carrieri³; Giulia Reis Minussi⁴; Guido Prandini Zambrana⁵; Jessica Seong Hyun Kang⁶; Rene Ramos de Oliveira⁷; Nelson Batista de Lima⁸; Ayrton Bernussi⁹; Juliusz Warzywoda¹⁰; and Antonio Hortencio Munhoz¹¹

Abstract: Pseudoboehmite is a hydrated aluminum oxyhydroxide obtained from inorganic precursors by the sol-gel process. It is used as a precursor to alumina and as a reinforcement in obtaining nanocomposites. Cement-reinforced composites with this nanomaterial were obtained in concrete and mortar. Pseudoboehmite with sodium polyacrylate was used to promote a deflocculation of pseudoboehmite particles, which tend to agglomerate in the material. The obtained material was added to the concrete to improve its workability and strength. The new concrete was characterized by slump tests and mechanical tests. Our results revealed that the incorporation of pseudoboehmite with sodium polyacrylate significantly increased the compressive strength and improved the workability of the concrete. Multiple experiments evaluated compressive strength, ultrasound speed, and nanomaterial characterization. Using the Weibull method in mortars, we verified that the pseudoboehmite brought visible benefits as the characteristic stress increased by 17.5%. This increase was observed with the addition of 3% by weight of pseudoboehmite. DOI: [10.1061/\(ASCE\)MT.1943-5533.0004586](https://doi.org/10.1061/(ASCE)MT.1943-5533.0004586). © 2022 American Society of Civil Engineers.

Author keywords: Nanomaterials; Pseudoboehmite; Concrete; Sodium polyacrylate; Mortar.

¹Associate Professor, School of Engineering, Mackenzie Presbyterian Univ., Rua da Consolação, 930, Consolação, São Paulo, SP 01302-907, Brazil. Email: caroline.pacheco@mackenzie.br

²Associate Professor, School of Engineering, Mackenzie Presbyterian Univ., Rua da Consolação, 930, Consolação, São Paulo, SP 01302-907, Brazil. Email: Renato.peres@mackenzie.br

³Civil Engineering Student, School of Engineering, Mackenzie Presbyterian Univ., Rua da Consolação, 930, Consolação, São Paulo, SP 01302-907, Brazil. Email: carrierigabi@gmail.com

⁴Civil Engineering Student, School of Engineering, Mackenzie Presbyterian Univ., Rua da Consolação, 930, Consolação, São Paulo, SP 01302-907, Brazil. Email: giuliaminussi@hotmail.com

⁵Civil Engineering Student, School of Engineering, Mackenzie Presbyterian Univ., Rua da Consolação, 930, Consolação, São Paulo, SP 01302-907, Brazil. Email: guido_prandini@hotmail.com

⁶Civil Engineering Student, School of Engineering, Mackenzie Presbyterian Univ., Rua da Consolação, 930, Consolação, São Paulo, SP 01302-907, Brazil. Email: jshkang11@gmail.com

⁷Técnico—Instituto de Pesquisas Energéticas e Nucleares, Ave. Professor Lineu Prestes, 2242, São Paulo, SP 05508-000, Brazil. Email: rolivier1969@gmail.com

⁸Tecnologista Senior III—Instituto de Pesquisas Energéticas e Nucleares, Ave. Professor Lineu Prestes, 2242, São Paulo, SP 05508-000, Brazil. Email: nblima@ipen.br

⁹Professor, Dept. of Electrical and Computer Engineering, Texas Tech Univ., Lubbock, TX 79409. Email: ayrton.bernussi@ttu.edu

¹⁰Senior Research Associate, Materials Characterization Center, Whitacre College of Engineering, Texas Tech Univ., Lubbock, TX 79409. ORCID: <https://orcid.org/0000-0002-3498-2028>. Email: juliusz.warzywoda@ttu.edu

¹¹Associate Professor, School of Engineering, Mackenzie Presbyterian Univ., Rua da Consolação, 930, Consolação, São Paulo, SP 01302-907, Brazil (corresponding author). ORCID: <https://orcid.org/0000-0002-4550-5294>. Email: ahmunhoz@yahoo.com

Note. This manuscript was submitted on November 16, 2021; approved on May 18, 2022; published online on November 26, 2022. Discussion period open until April 26, 2023; separate discussions must be submitted for individual papers. This paper is part of the *Journal of Materials in Civil Engineering*, © ASCE, ISSN 0899-1561.

Introduction

Green concretes have been considered an environmentally friendly alternative solution for conventional concrete, which can be prospectively manufactured with less energy consumption and reduced generation of carbon dioxide (Vishwakarma and Ramachandran 2018). The reduction of cement consumption is also motivated by the prospect of developing new materials that can replace, at least in part, the total aggregates of concrete (sand and cement). In addition, alternative concrete materials that can be used to minimize illegal extraction, material scarcity, high costs, and exposure to health issues are critical.

Among the proposed approaches to realize green concretes, those incorporating nanoparticles in their composition are particularly important. Nanoparticle addition in normal-weight concrete revealed that the single addition of nanosilica, nano hematite, and nanotitania particles and their combination up to 2.0% by weight improved their physical properties, compressive strength and durability, and gamma radiation attenuation (Al-Tersawy et al. 2021; Xiao et al. 2021). The addition of graphene oxide and nanofibrillated cellulose in concrete showed that nanostructures furthered the cementitious matrix's homogeneity, affected the electrical resistance of the high-frequency arc, and influenced the matrix porosity, which was verified by compressive strength measurements (Silva et al. 2021). Increased compressive strength of mortar in M-Sand, an eco-friendly alternative to natural sand cement mortar, was determined by incorporating alpha-phase nanoalumina (Alex et al. 2021). The replacement of portland cement with nanomontmorillonite powder resulted in up to a 1.5% increase in compressive, tensile, and flexural strengths. In addition, the microstructure changed due to the filler nucleation effect that increased the cement hydration rate (Kafi et al. 2016).

Although there have been few previous reports dedicated to the study of green concretes, detailed investigations on the effects of nanomaterials added to the concrete on its mechanical properties

remain largely unexplored. In particular, the incorporation of pseudoboehmite and sodium polyacrylate in concretes have not been studied thus far. Sodium polyacrylate is an efficient deflocculant for ceramic suspensions with a high solids concentration and will be used to prevent the agglomeration of pseudoboehmite nanoparticles (Leong et al. 1995). In this work, we performed detailed investigations on the mechanical properties of concrete incorporating pseudoboehmite nanoparticles and sodium polyacrylate at different concentrations. Our results revealed enhanced mechanical strength to compression and workability and improved homogeneity in concrete samples containing pseudoboehmite nanoparticles and sodium polyacrylate.

Methodology

Concrete

The pseudoboehmite synthesized by the sol-gel process was added to the concrete along with sodium polyacrylate at different concentrations. The obtained concrete was characterized using various experiments to verify its mechanical properties, porosity, and workability.

For the mix of pilot concrete, cement–sand–gravel mass proportions of 1:2:3 were used with a water-cement ratio of 0.62 (Neville 2006). For the analysis of pseudoboehmite effect in concrete, six traces were obtained: Trace 0 without the addition of pseudoboehmite and sodium polyacrylate, Traces 1F, 2F, 3F, and 4F were prepared with different pseudoboehmite concentrations, and 5F corresponds to a trace in which sodium polyacrylate and pseudoboehmite were solubilized in water and mixed with cement–sand–gravel according to Table 1. The sodium polyacrylate was added to the pseudoboehmite gel, and the mixture was used to produce the concrete in 1F, 2F, 3F, and 4F.

The factorial 2^2 experimental design calculated the concrete traces (Box et al. 1978). The variables are the addition of pseudoboehmite and sodium polyacrylate. The levels of 2^2 factorial experimental design variations are listed in Table 2.

Mortar

The molding of the specimens was carried out using a mortar trace 1.0:3.0:0.48 (cement-sand-water), and the cement used was portland cement, CP IV-32. The mortar was prepared using a mechanical mixer. First, all the sand and a small amount of water were mixed to minimize material loss during the process. Then, the cement and the remaining water were added and mixed. For the

specimens incorporating pseudoboehmite, pseudoboehmite was added last. In total, 15 test specimens with 50-mm diameter and 100-mm height were molded, as shown in Fig. 1.

Before starting the molding, the release agent was applied internally. The process was carried out in four layers with approximately equal heights, where each layer received 30 hits to remove any air bubbles. The specimens were molded with 0%, 1%, and 3% by weight of pseudoboehmite calculated based on cement mass.

Characterization of Pseudoboehmite

The pseudoboehmite samples used in the concrete experiments were characterized using different experiments. First, the thermal analysis used a gel sample. Differential thermal analysis (DTA) and thermogravimetric analysis (TGA) were performed using Netzsch equipment (Gebrüder-NETZSCH-Straße, Selb, Germany), model S.T.A. 449F3-Jupiter. A quantity of 0.013 g of sample was placed in an open alumina crucible, and DTA-TG measurements were performed simultaneously. The samples were heated from room temperature to 1,300°C at a rate of 10°C min⁻¹ using a nitrogen flow of 60 mL min⁻¹.

The pseudoboehmite gel was analyzed by the Zeta potential technique to evaluate whether the gel particles' dispersion was stable. Measurements were performed using LitesizerTM equipment (Anton Paar, Graz, Austria) at room temperature. First, 0.1 g of pseudoboehmite was added to 100 mL of distilled water. The suspension was maintained on an ELMASONIC P ultrasound (ELMASONIC, New York) for 30 min, and then the measurement was performed. The analyses were repeated twice for reliability verification purposes.

The gel was frozen and freeze-dried for the other analyses using Terroni equipment (Terroni, São Carlos, Brazil). Then, the pseudoboehmite powder was analyzed by X-ray diffraction to verify the phases present in the sample using a Rigaku MultiFlex diffractometer powder (Rigaku, Tokyo) with CuK α radiation ($\lambda = 1.542 \text{ \AA}$) under 40 KV voltage and 20 mA current. The scanning angle (2θ) was varied from 0° to 90° using a 2° min⁻¹ scan.

Pseudoboehmite powder adsorption isotherms were performed to evaluate the presence of mesopores, micropores, and macropores

Table 1. Factorial design matrix of two variables

Dash	A	B
1F	–	–
2F	+	–
3F	–	+
4F	+	+

Table 2. Formulation of four different variations of the pilot trace

Variables	Level (–) (% by weight)	Level (+) (% by weight)
A: addition of pseudoboehmite ^a	1	5
B: addition of sodium polyacrylate in the pseudoboehmite ^a	0	1

^aCalculated based on cement mass.

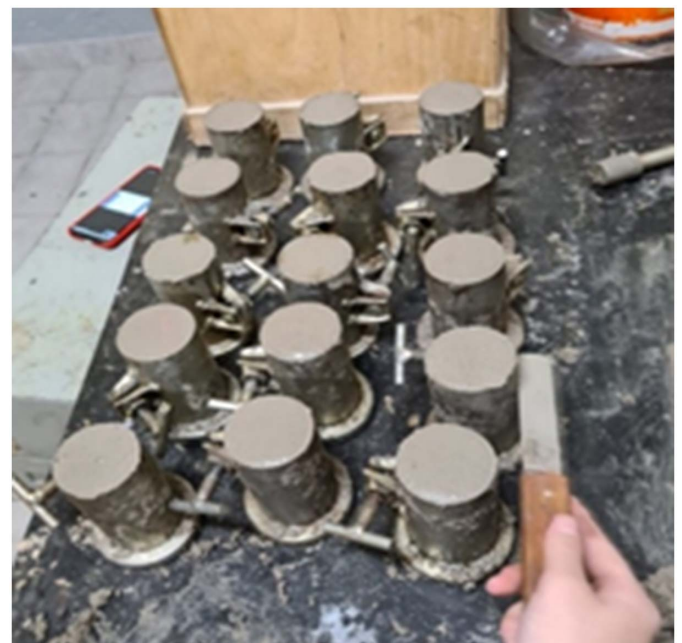


Fig. 1. Mortar specimens (diameter = 50 mm; height = 100 mm).

in the sample and measure the specific surface area of pseudoboehmite using the Brunauer Emmett Teller (BET) method.

The adsorption and nitrogen desorption isotherms were determined using Belsorp Max equipment (Belsorp Max, Osaka, Japan). The samples were previously degassed at 100°C for a period of 24 h. The BET method determined the specific surface area from the nitrogen adsorption isotherms acquired at 77 K.

The scanning electron microscopy (SEM) technique evaluated the morphology of synthesized pseudoboehmite particles. SEM images were obtained using a JEOL JSM-6510 microscope (Jeol, Massachusetts). The samples used for SEM analyses were placed in a sample port (stubs) and coated with gold using the sputtering technique. The micrographs were obtained using a secondary electron detector. The samples were also analyzed by scanning electron microscopy using an energy-dispersive X-ray spectroscopy (EDS) detector.

Transmission electron microscopy (TEM) of pseudoboehmite particles was realized using a transmission electron microscope Hitachi H-9500 (Hitachi, Japan). The samples were dispersed in ethanol using an ultrasound bath before supporting them in the copper grid covered with formvar.

Standard Method for Pulse Velocity through Concrete

The ultrasonic wave propagation velocity method was used to verify the homogeneity and porosity of the fabricated concrete. The higher the wave propagation velocity, the more homogeneous the concrete is. In contrast, the lower the wave propagation velocity, the more porous the concrete is likely to be. The ultrasound method is based on the idea that longitudinal pulse waves travelling through the material depend on its elastic properties and density. Ultrasound tests were performed using the ASTM C597-16 (ASTM 2016) Proceq equipment (Pundit model) (Proceq equipment, São Paulo, Brazil).

Determination of Compressive Strength

The specimens were tested to determine the axial compressive strength (Fig. 2). The samples were fractured at 7, 14, 21, 28, and

60 days of age using the Amsler compression test machine (universal model) (Germany).

In the compression test, the load application faces of the specimens (bottom and top) must be rectified following that prescribed by the ABNT NBR 5739 (BS 2018) standard test method in the case of molded samples. Under the test conditions, the distance between the vertical axis of the machine and the test body axis, measured at its ends, shall be at most 1% of its nominal diameter, the diameter used for calculating the cross-sectional area shall be determined, with an accuracy of ± 1 mm, by the average of two diameters measured orthogonally at half the height of the test body. Specimens must be broken to compression at a given specified age. In the samples molded, the period must be counted from when the cement is in contact with the mixing water. The load plates' facets and the specimen must be cleaned and dried before the test body is placed in a test position. The test body must be carefully centered on the lower plate, with the reference concentric circles. The force scale chosen for the trial shall be such that the test body's rupture must occur with a load within 10% to 90% of the scale range. The test load should be applied continuously and without shocks, with a loading speed of 0.05 MPa/s. No adjustment should be made to the machine controls when the test body is rapidly deforming as it approaches its rupture. In the case of machines provided with analogue load indication, charging shall only cease when the load pointer's recoil is around 10% of the maximum load value achieved, which shall be noted as a rupture load of the test body.

Synthesis of Pseudoboehmite

The sol-gel process was used in the synthesis of pseudoboehmite. This preparation methodology, which has attracted much interest from industries since the 1970s, involves the formation of a suspension of very fine particles of colloidal size dispersed in a liquid (sol) and its transformation into a continuous network (gel); the process is easily carried out at low temperatures. Therefore, this process can be mass-produced conveniently at room temperature, and it is the feasibility of practical engineering for future applications.

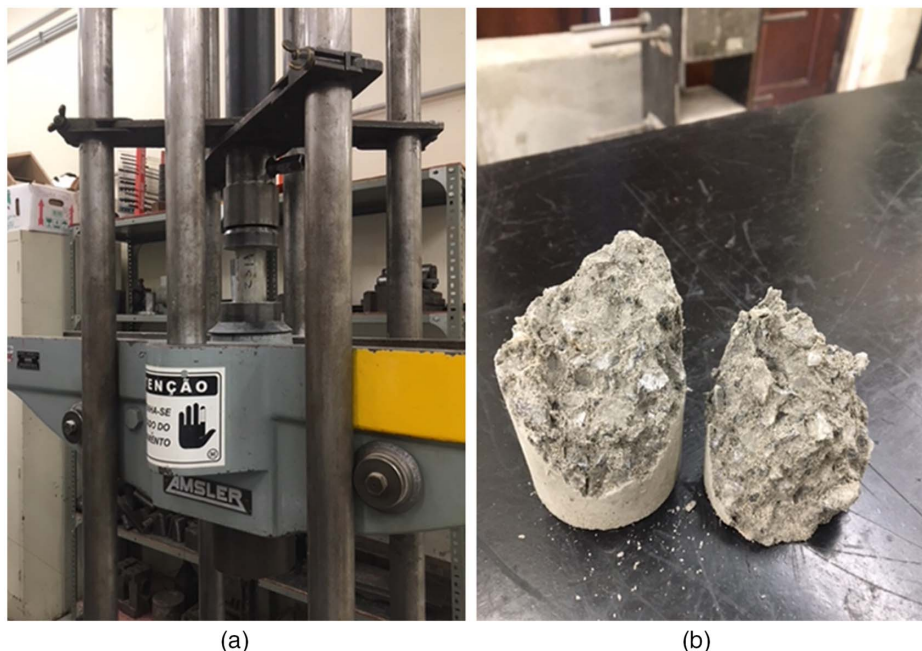


Fig. 2. Compressive strength: (a) Amsler compression test machine; and (b) fractured specimen of Sample 4F.

The aqueous solution of AlCl_3 anhydrous (P.A. Sigma-Aldrich Handels, Vienna, Austria), precursor, and ammonium hydroxide (NH_4OH) (28%–30% by weight NH_3) (Sigma-Aldrich supplier) were the reagents used in the synthesis (Munhoz et al. 2012). First, anhydrous aluminum chloride was dissolved in distilled water, and then the aluminum chloride solution was dripped into the ammonium hydroxide solution. Then, the precipitate obtained in the Buchner funnel with a vacuum pump was filtered and washed with distilled water. Next, the gel remaining in the Buchner funnel was washed with distilled water to remove the excess of NH_4OH and by-products of the reaction until the pH of the filtrate was equal to 7.

Results

Zeta Potential Measurements of Pseudoboehmite

The Zeta potential was determined for the products (gel) of two different batches. First, the gel obtained was washed with distilled water until the pH of the filtrate reached 7. Then, the sample was prepared on ultrasound, and the Zeta potential was determined. The Zeta potential analysis of pseudoboehmite gel provided mean values of -41.3 mV (Fig. 3) and -41.6 mV, indicating a stable dispersion. We observed that different batches of pseudoboehmite synthesis resulted in Zeta potential values near -41 mV. Thus, the similar Zeta potential results provide compelling evidence of the

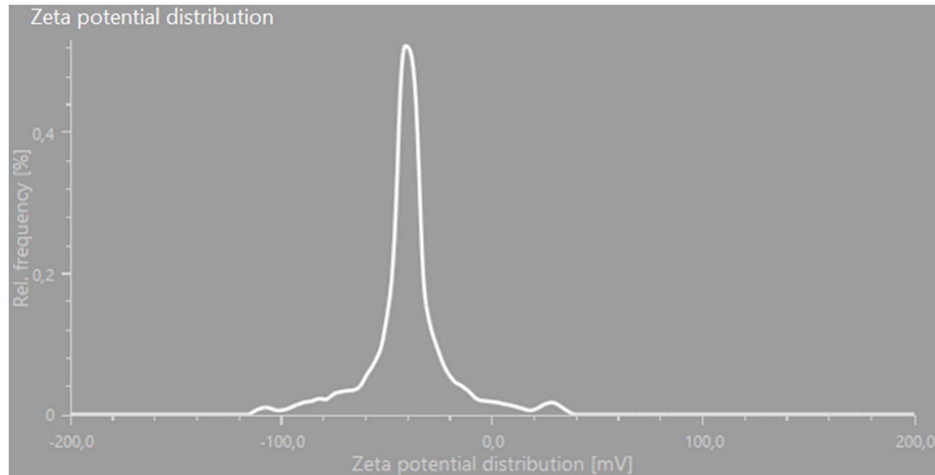


Fig. 3. Zeta potential analysis of the synthesized pseudoboehmite gel for the first batch sample.

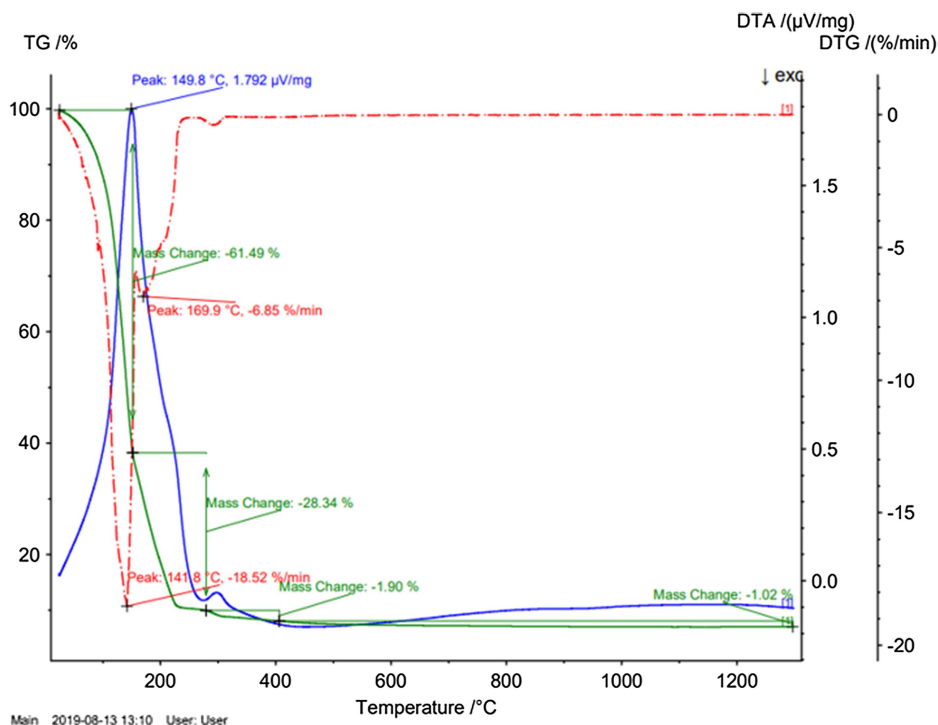


Fig. 4. DTA, TG (curve with the mass change annotations), and DTG (dotted line) of pseudoboehmite sample.

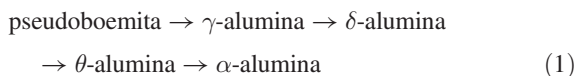
synthesized pseudoboehmite gel process reproducibility used in this work.

These Zeta potential results are also a clue that the agglomeration of the gel particles would not be possible. Furthermore, sodium polyacrylate was also used to avoid pseudoboehmite particles agglomeration, according to the literature (Leong et al. 1995). Therefore, the Zeta potential and sodium polyacrylate addition is also a clue that the distribution of the pseudoboehmite particles in the concrete and mortar is homogeneous.

DTA and TGA Analysis of Pseudoboehmite Gel

The results obtained from the gel's thermal analyses, DTA and TGA, are observed as the first endothermic peak associated with the loss of mass of water. For pseudoboehmite samples, a second mass loss related to pseudoboehmite transformation into gamma-alumina is observed above 200°C (Fig. 4). In thermogravimetry and DTG, mass loss around 100°C was observed due to water evaporation and 169.9°C in the DTG (dashed line), a second mass loss associated with pseudoboehmite transformation into gamma-alumina (Munhoz et al. 2012).

With increasing temperature, the different alumina phases are formed according to Eq. (1). The phase transition is not reversible (Munhoz et al. 2012; Moroz et al. 2006). Considering the curing process of concrete and mortar did not reach 50°C, much less than 200°C observed in DTA and TG for the transformation of pseudoboehmite in gamma-alumina, the phase present in concrete and mortar is the pseudoboehmite



Pseudoboehmite X-Ray Diffraction Data

A representative X-ray diffraction pattern from a pseudoboehmite sample is shown in Fig. 5. The diffraction peaks' positions are consistent with previous reports (Musić et al. 1999; Moroz et al. 2006). The results in Fig. 5 show that the samples exhibited a pronounced diffraction line broadening due to small crystallite dimensions. It is impossible to differentiate this phase from pseudoboehmite, beta boehmite, and alpha boehmite. Therefore, we have assumed it generically as boehmite.

Nitrogen Absorption and Specific Surface Area of Pseudoboehmite

Fig. 6 shows the absorption isotherm obtained for a pseudoboehmite sample, corresponding to a Type IV isotherm. A Type IV

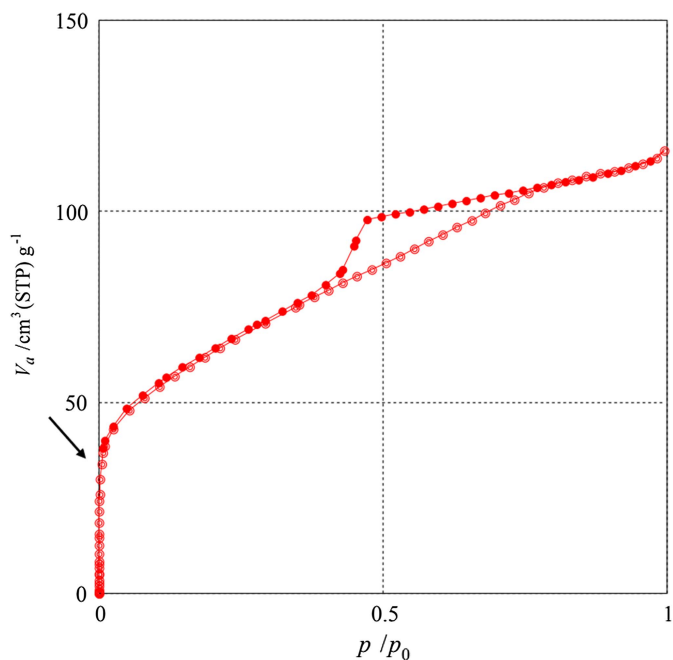


Fig. 6. Absorption isotherm of a pseudoboehmite sample.

isotherm is characteristic of materials with macropores and mesopores. It probably also presents micropores as observed at the beginning of adsorption isotherms (solid arrow on the left of Fig. 6). The volume adsorbed at the beginning of the isotherm, where $p/p_0 \sim 0$, indicates the presence of micropores. The hysteresis shown in the isotherm curves corresponds to Type H2, which is usually associated with capillary condensation in mesoporous structures. Type H2 hysteresis is typical for inorganic oxides with a complex network of interconnected narrow pores whose pore-size distribution and shape are not well defined (Sing et al. 1985).

Fig. 7 shows the BET plot, and the result was 218.5 m²/g. The specific surface area of 218.5 m²/g shows a large area of the nanomaterial that could be dispersed in the cement composites and would collaborate to improve the mechanical resistance.

Scanning Electron Microscopy of Pseudoboehmite

Fig. 8 shows a representative SEM micrograph image of a pseudoboehmite sample using a secondary electron detector. The image reveals clusters formed by individual particles in the form of plates. This result is consistent with previous reports of nanoparticles of

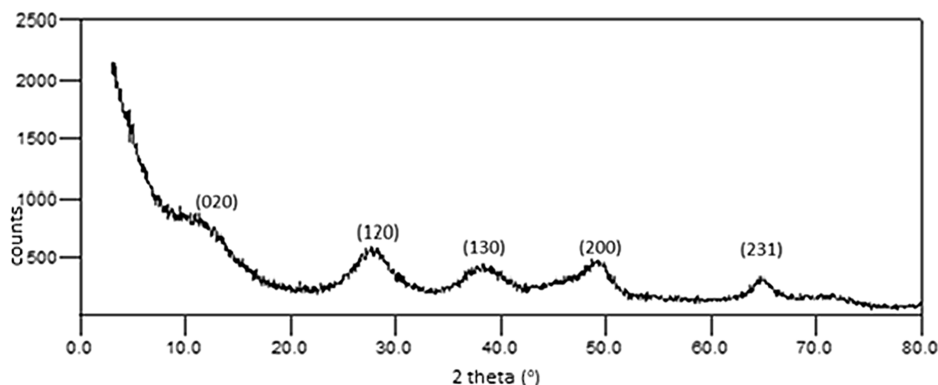


Fig. 5. X-ray diffraction pattern of the synthesized pseudoboehmite sample.

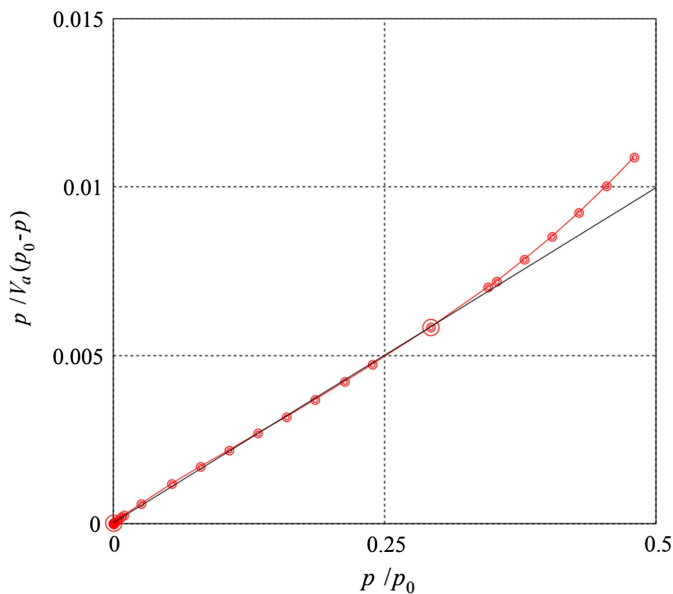


Fig. 7. Specific surface area of 218.5 m²/g by the BET method.

pseudoboehmite (Musić et al. 1998, 1999). The semiquantitative EDS results show a composition of approximately two oxygens for one aluminum, which is according to the pseudoboehmite chemical formula (AlOOH)_n·xH₂O.

Fourier Transform Infrared Spectroscopy Spectrum of Pseudoboehmite

The Fourier transform infrared spectroscopy (FTIR) transmission spectrum of a pseudoboehmite sample is shown in Fig. 9. Absorption peaks were observed that are typical of boehmite (Ram 2001). The very strong and broadband centered near 3,400 cm⁻¹ with no shoulders is characteristic of the not-well-crystallized

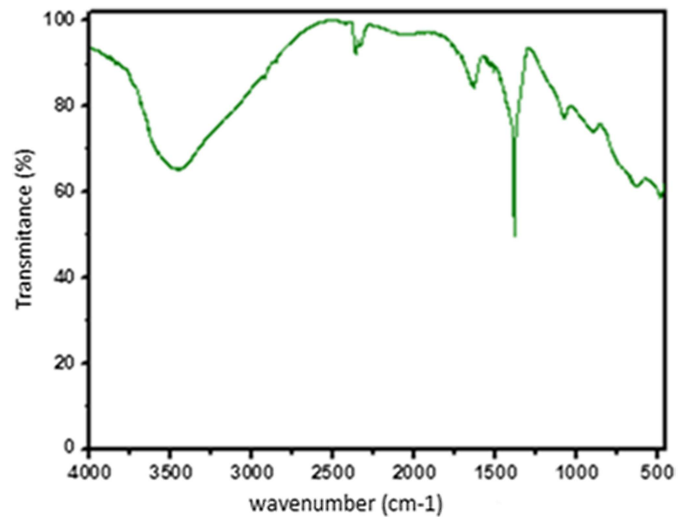


Fig. 9. FTIR transmittance spectrum of a pseudoboehmite sample.

pseudoboehmite with nanoparticles (Musić et al. 1999). Because the highest frequency band is the next 1,650 cm⁻¹ is always present in nanocrystals, according to Ram (2001), the results are consistent. The shoulders at the high energy side of the hydroxyl bands at around 3,400 cm⁻¹ were due to adsorbed water in well-crystallized material.

At high wave numbers, a very strong and broadband centered at 3,441 cm⁻¹ is present. When shoulders at around 3,307 and 3,101 cm⁻¹ are observed, they are due to the sample's long auto-claving time, which allows the formation of well-crystallized boehmite with a reduced specific surface area. Due to nanoparticles in the sample, there were no shoulders in the FTIR transmission spectrum (Fig. 9). Thus, the results of the FTIR analysis agree with the results of the transmission electron microscopy and the specific surface area.

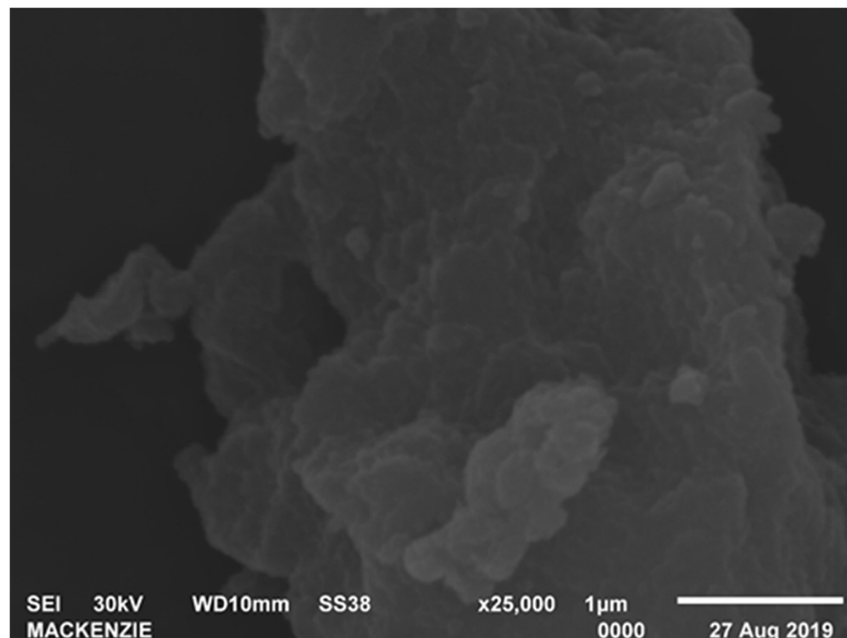


Fig. 8. SEM image of a pseudoboehmite sample.

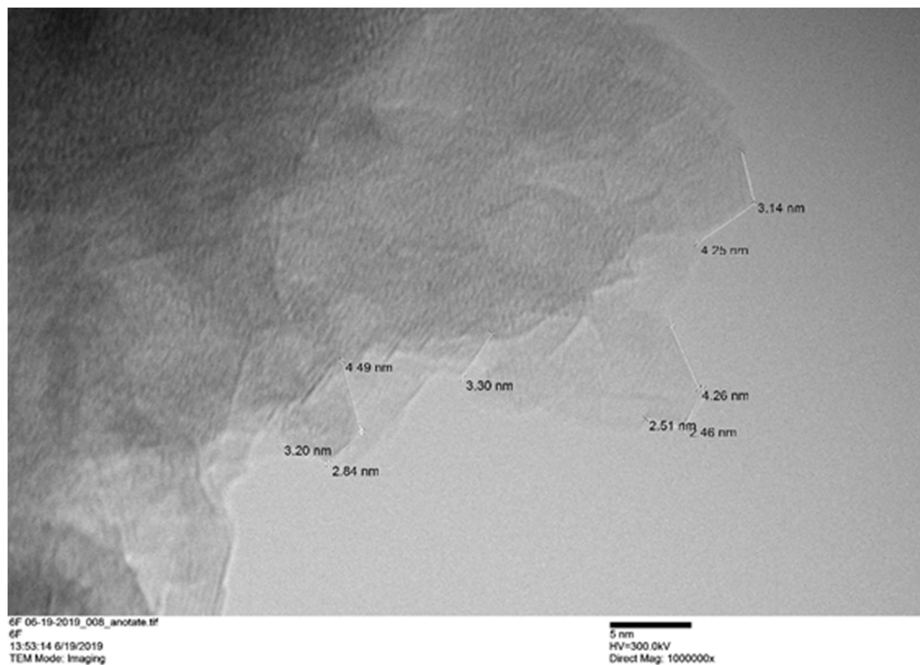


Fig. 10. TEM image of an aggregate of pseudoboehmite nanoparticles.

Transmission Electron Microscopy of Pseudoboehmite Samples

Fig. 10 shows the TEM image of a pseudoboehmite sample at the edge of an aggregate of pseudoboehmite nanoparticles. The particles, consisting of tiny plates in the range of colloidal dimensions, are anisometric, with a lateral size smaller than 5 nm. At the edges of the aggregate where the individualized particles were observed, the particle and the region immediately adjacent (void) had a very close intensity contrast, showing that the particles are thin (probably <1 nm), in agreement with previous reports (Musić et al. 1998, 1999). The results are consistent with the SEM, X-ray diffraction, and FTIR analysis. The aggregation of particles was previously observed by de Aguilar Cruz and Eon (1998) for unaged pseudoboehmite. The high specific surface area and consequently the high surface energy promotes the growth of particles or the aggregation of nanoparticles in the drying process (Cao and Wang 2011).

Analysis of the Concrete Incorporating Pseudoboehmite Nanoparticles and Polyacrylate

The results obtained in the characterization of the concretes are presented in this section. The tests were performed for concrete obtained with the dashes in Table 3.

Table 3. Dashes

Dash	Composition
0	Reference
1F	1% by weight pseudoboehmite
2F	5% by weight pseudoboehmite
3F	1 % by weight pseudoboehmite + polyacrylate (10 g) ^a
4F	5% by weight pseudoboehmite + polyacrylate (10 g) ^a
5	1% by weight pseudoboehmite + polyacrylate (10 g) (dissolved in water)

^aSodium polyacrylate mixture in pseudoboehmite gel.

Abatement of the Cone Trunk

After mixing, the cone trunk abatement test was performed to evaluate the workability of the concrete, according to Fig. 11.

It was observed that the addition of pseudoboehmite with sodium polyacrylate improved workability (Fig. 11) when compared with Trace 0. However, we determined that adding 5% by weight pseudoboehmite (Samples 2F and 4F) promoted a more expressive increase in the abatement result, providing better workability of the concrete. The addition of a gel containing nanoparticles promotes plasticity in the concrete. Dash 2F has no sodium polyacrylate.

Axial Compression Resistance Test for Concrete

Axial compressive strength tests were performed, and the results are presented in Fig. 12. The addition of sodium polyacrylate and pseudoboehmite increased the effects of compressive strength. However, the increase in axial compressive strength in the concrete with pseudoboehmite and polyacrylate was lower than that obtained in cement paste with the addition of nano-SiO₂, nano-TiO₂, and

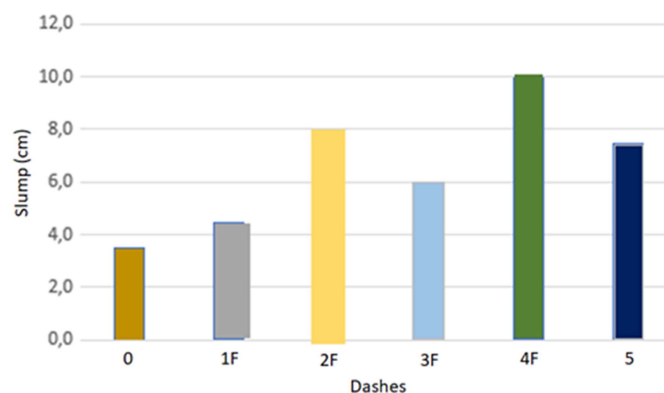


Fig. 11. Cone abatement results for different dashes.

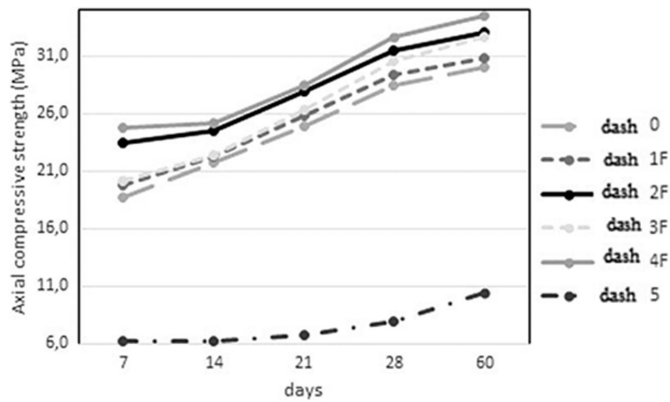


Fig. 12. Results of the compression strength (MPa) assay.

nano- Al_2O_3 particles previously reported (Al-Tersawy et al. 2021; Xiao et al. 2021; Alex et al. 2021). This result is probably due to the small Young's modulus of pseudoboehmite compared with nano- SiO_2 , nano- TiO_2 , and nano- Al_2O_3 .

With the addition of pseudoboehmite and sodium polyacrylate, it was observed that there was an improvement in mechanical resistance to compression compared with Trace 0. Again, the addition of 5% by weight pseudoboehmite promoted the most expressive increase in compressive mechanical resistance.

The effect of sodium polyacrylate in pseudoboehmite has been reported in the literature. The agglomeration state of boehmite particles is avoided due to the formation of a complex between the boehmite surface and carboxylate groups of sodium polyacrylate, thus preventing particles from coalescence with each other (Mathieu 2008). As the precursor in the synthesis, aqueous aluminum chloride salt solution, the pseudoboehmite was obtained. After a treatment with sodium polyacrylate to avoid the aggregation of the particles, stable colloidal suspensions of pseudoboehmite nanoparticles were obtained (Mathieu 2007).

For the sample where sodium polyacrylate was dissolved in water (Trace 5), we observed that the mechanical compressive strength data were the worst.

Sodium polyacrylate is a superabsorbent polymer with great affinity with water, and osmotic pressure causes sodium polyacrylate to water to balance the sodium ion concentration inside and outside the polymer. The sodium polyacrylate in this experiment probably absorbed the water, avoiding the hydration in concrete

products, resulting in lower mechanical compressive strength. Even for a high curing time of 60 days, we determined that the mechanical strength of compression of this trace was much lower when compared with the others. Only Trace 5 exhibited a mechanical resistance value lower than the reference dash without the addition of pseudoboehmite and sodium polyacrylate.

Ultrasonic Wave Propagation Speed

The ultrasonic wave propagation velocity was obtained for different aged concretes. According to the classification table of concretes based on the propagation speed of the ultrasonic wave (Tam et al. 2018), for $v \geq 4,500$ m/s, the concrete is considered excellent. Except for Trace 5, all dashes with ultrasonic wave propagation velocity are above 4,500 m/s.

Fig. 13 illustrates the corresponding results of traces and the propagation velocity of the ultrasonic wave results (m/s).

According to reported data (Daoud and Al-Nasra 2014; Manzur et al. 2015), the addition of sodium polyacrylate promotes the workability of concrete. The sodium polyacrylate within concrete creates additional voids that generally lessen the concrete strength but improve workability and consistency. According to Niewiadomski (2015), silica and alumina nanoparticles promote the workability of the concrete mixture. The structure of concrete that contains nanoparticles was much more compact than that of concrete without nanoparticles. The results of ultrasonic wave propagation (Fig. 13) show that the pseudoboehmite and sodium polyacrylate addition promoted an increased ultrasonic wave propagation velocity and the homogeneity of the concrete. The ultrasonic wave propagation velocity and the Zeta potential of pseudoboehmite are a clue of the homogeneous distribution of the pseudoboehmite in concrete.

According to literature (Kumar Mehta and Monteiro 2013), the ultrasound test's speed allows for the concrete's homogeneity. The higher the wave's velocity, the better the concrete's compactness and homogeneity. The increase in the propagation speed of concrete with the addition of pseudoboehmite and sodium polyacrylate indicates that the concrete became more homogeneous than a block of concrete of Dash 0.

The synergic effect of pseudoboehmite and sodium polyacrylate promoted the workability and improved the axial compression strength (Figs. 12 and 13). In addition, the pseudoboehmite nanoparticles probably contributed to the reduction of concrete porosity. The increase in the propagation speed of concrete was also associated with reducing porosity. The addition of nanoparticles in

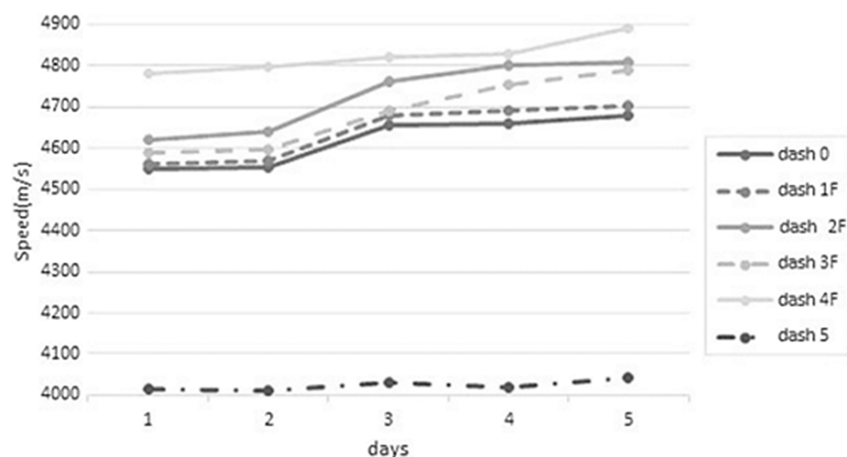


Fig. 13. Ultrasonic wave propagation velocity (m/s) for different aged concretes.

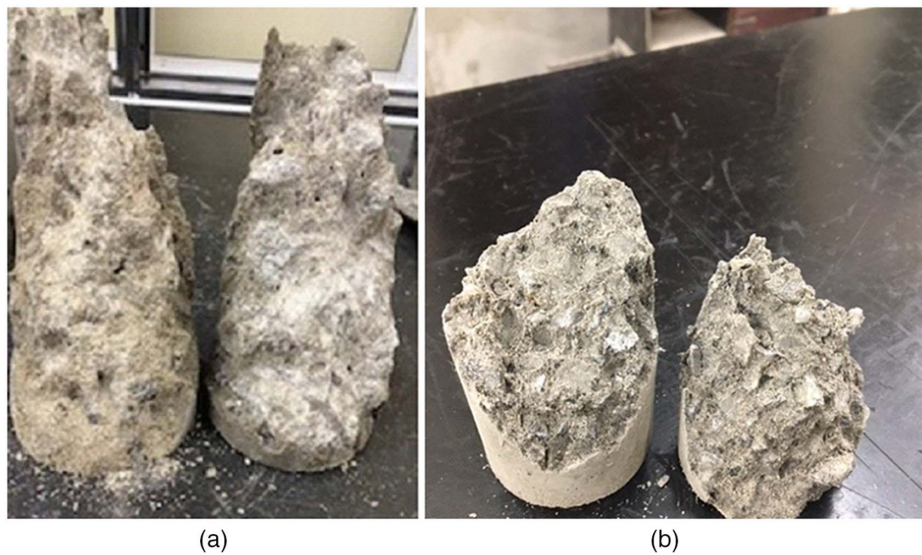


Fig. 14. Fractured concrete of (a) Dash 0; and (b) Dash 4F.

concrete reduced the porosity, as reported in the literature (Silva et al. 2021).

Fig. 14 shows fractured concrete of Dash 0 and Dash 4F. It appears that a more tortuous crack path is observed in the sample of Dash 4F that contains sodium polyacrylate the pseudoboehmite. The crack in Dash 0 makes it look more plane than Dash 4F.

Fig. 13 is consistent with the mechanical and compressive strength measurements.

The mechanical resistance exhibited the same tendency, except for Trace 5, whose mechanical resistance and ultrasonic wave speed were below the other traces. Only Trace 5 presented a much lower mechanical strength value than others, probably due to the absorption of the water by the sodium polyacrylate that inhibited the cement hydration rate. This experiment's water-cement ratio of 0.62 was the same as the other dashes.

Axial Compression Resistance Test for Mortar

Table 4 lists the results of the compression tests carried out at 7 days for the specimens without the addition of pseudoboehmite, with 1% and 3% by weight of pseudoboehmite.

Due to the COVID pandemic problem, the laboratory was closed, and the other specimens were only tested after 42 days. Table 5 lists the results of the compression tests carried out at 42 days for the specimens without the addition of pseudoboehmite, with 1% and 3% by weight of pseudoboehmite.

Using the Weibull method for the data of proof bodies (specimens) in Table 5, the graph shown in Fig. 15 was drawn. Then, calculating the Weibull modulus and the characteristic stress, the

Table 4. Axial compressive strength (MPa) results at 7 days

Sample	Proof bodies (specimens) without pseudoboehmite	Proof bodies (specimens) containing 1% by weight pseudoboehmite	Proof bodies (specimens) containing 3% by weight pseudoboehmite
CP1	16.45	15.08	11.49
CP2	15.25	16.53	14.05
CP3	14.52	17.43	14.53

values are given in Table 6. These compression strength values are typical for mortar (Itim et al. 2011; Yeon 2021).

Comparing the specimens without the addition of pseudoboehmite with the one containing 3% by weight by mass of pseudoboehmite (Table 6), it is verified that there was an increase in the characteristic stress by 17.5%. This increase is considerable, given the small amount of pseudoboehmite added.

For 3-day measurements, the compressive strain results were similar. However, the Weibull method could not determine the characteristic axial compression strength due to the small number of samples analyzed.

After analyzing the results obtained for 42 days, we verified that the addition of pseudoboehmite at a concentration of 3% by weight improved the mechanical compression strength compared with specimens without the pseudoboehmite addition. However, for the samples in which only 1% by weight of pseudoboehmite was added, we determined that the compression strength was lower than those without the pseudoboehmite addition. Therefore, adding 1% of pseudoboehmite was probably insufficient to improve the axial compressive strength.

In a study with different types of nanoparticles incorporated into the mortar, namely nano-SiO₂, nano-TiO₂ and nano-Fe₂O₃, it was also observed that with 3% by weight, there were the best results for mechanical strength compared with 1% by weight (Ng et al. 2020).

Table 5. Axial compressive strength (MPa) results at 42 days

Sample	Proof bodies (specimens) without pseudoboehmite	Proof bodies (specimens) containing 1% by weight pseudoboehmite	Proof bodies (specimens) containing 3% by weight pseudoboehmite
CP1	29.98	24.29	31.12
CP2	27.14	26.05	36.99
CP3	31.35	23.31	35.43
CP4	29.41	25.26	33.78
CP5	30.09	24.98	35.03
CP6	31.05	24.79	28.97
CP7	27.53	25.04	32.99
CP8	28.63	25.02	37.45
CP9	30.48	24.48	36.05

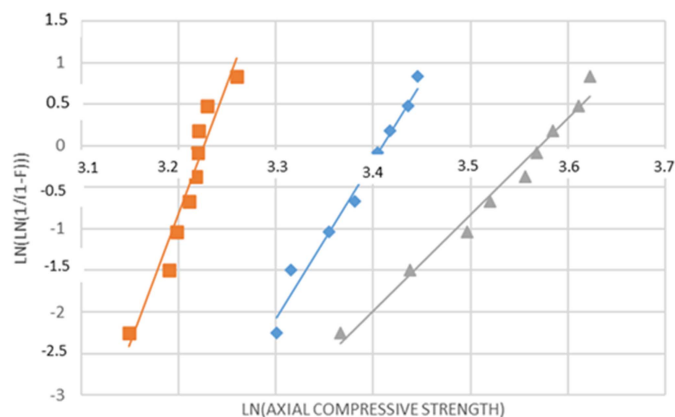


Fig. 15. Weibull method applied to mortar data. F = probability of failure; small square = mortar data without pseudoboehmite; large square = mortar with the addition of 1% by weight of pseudoboehmite by mass; and triangle = mortar with the addition of 3% by weight of pseudoboehmite by mass.

Table 6. Characteristic axial compressive strength (MPa) and Weibull modulus results at 42 days

Samples	Characteristic axial compressive strength (MPa)	Weibull modulus
Mortar data without pseudoboehmite	30.3	19.1
Mortar with the addition of 1% by weight pseudoboehmite	25.2	31.1
Mortar with the addition of 3% by weight pseudoboehmite	35.6	11.6

The addition of nanoparticles in mortar increases the rate of hydration of cement. In addition, due to their small size, it provides additional nucleation sites for the precipitation and development of calcium silicate hydrates (C-S-H). The nano-C-S-H is the main binding phase in all portland cement-based systems, and their bonding to other hydration products is generally reasonable. In addition, the nanoparticles reduce the amount of free water, reducing the porosity of the mortar.

The Weibull modulus, m , measures the scatter of the axial compressive strength data—the wider the distribution, the smaller m (Davidge 1980; Richerson 1992). Comparing the Weibull modulus, we determined $m = 19.1$ without the addition of pseudoboehmite. In contrast, $m = 31.1$ and $m = 11.61$ were determined for 1% and 3% by weight addition of pseudoboehmite, respectively. The m results showed that the specimens with 1% by weight of pseudoboehmite had a more similar axial compressive strength than those with 3% by weight of pseudoboehmite. However, values of $m = 11.61$ already indicate a homogeneous distribution of compressive strength values, also indicating that the microstructure and distribution of pseudoboehmite particles in the mortar were also homogeneous. These data and the Zeta potential of pseudoboehmite are clues that the pseudoboehmite was homogeneously distributed in the specimens.

Conclusions

In this research, pseudoboehmite was synthesized by a sol-gel process. In addition, the effects of different dosages of pseudoboehmite nanoparticles on mortar and concrete have been investigated.

The purity of pseudoboehmite nanoparticles was verified by DTA, TG, and X-ray diffraction experiments. Furthermore, the nano dimension was observed in TEM. In addition, the Zeta potential results confirmed the dispersion's stability. Finally, pseudoboehmite and sodium polyacrylate were added to the concrete. Our results revealed an increase in the ultrasound speed propagation, suggesting an increasing homogeneity of the molded concrete specimens and an increase in mechanical strength to compression and the workability of the concrete. These results further confirm that the addition of pseudoboehmite nanoparticles and sodium polyacrylate enhances the physical characteristics of the concrete. Furthermore, in mortar specimens, adding 3% by weight of pseudoboehmite increased the characteristic compression strength using the Weibull method by 17.5%. This increase in compression strength may be due to the high surface activity of nanoparticles that increased the rate of hydration of cement, promoting a more uniform distribution of hydration products causing denser packing of the particles and reducing the porosity of mortar.

Data Availability Statement

All data, models, and code generated or used during the study appear in the published article.

Acknowledgments

The authors thank Mackenzie Presbyterian University, Mack Pesquisa, Cnpq, and FAPESP (Grant Nos. 2010/19157-9 and 2017/22396-4) for the sponsorship of this project.

References

- Alex, A. G., T. Gebrehiwet, and Z. Kemal. 2021. "M-Sand cement mortar with partial replacement of alpha phase nano alumina." *J. Build. Rehabil.* 6 (21): 17. <https://doi.org/10.1007/s41024-021-00111-8>.
- Al-Tersawy, S. H., R. A. El-Sadany, and H. E. M. Sallam. 2021. "Long-term behaviour of normal weight concrete containing hybrid nanoparticles subjected to gamma radiation." *Arch. Civ. Mech. Eng.* 21 (4): 9. <https://doi.org/10.1007/s43452-020-00157-4>.
- ASTM. 2016. *Red standard test method for pulse velocity through concrete*. ASTM C597-16. West Conshohocken, PA: ASTM.
- Box, G. E. P., W. G. Hunter, and J. S. Hunter. 1978. *Statistics for experimenters—An introduction to design, data analysis and model building*. New York: Wiley.
- BS (Brazilian Standards). 2018. *Concrete compression test of cylindrical specimens*. ABNT NBR 5739. São Paulo, Brazil: BS.
- Cao, G., and Y. Wang. 2011. *Nanostructures and nanomaterials—Synthesis, properties and applications*. New York: World Scientific.
- Daoud, M., and M. Al-Nasra. 2014. "The use of super absorbent polymer as a sealing agent in plain concrete." *Am. J. Eng. Res.* 3 (3): 132–137.
- Davidge, R. W. 1980. "Mechanical behaviour of ceramics." In *Cambridge solid state science series*. Cambridge, UK: Cambridge University Press.
- de Aguilar Cruz, A. M., and J. G. Eon. 1998. "Boehmite-supported vanadium oxide catalysts." *Appl. Catal., A* 167 (12): 203–213. [https://doi.org/10.1016/S0926-860X\(97\)00316-5](https://doi.org/10.1016/S0926-860X(97)00316-5).
- Itim, A., K. Ezziane, and K. El-Hadj. 2011. "Compressive strength and shrinkage of mortar containing various amounts of mineral additions." *Constr. Build. Mater.* 25 (8): 3603–3609. <https://doi.org/10.1016/j.conbuildmat.2011.03.055>.
- Kafi, M. A., A. Sadeghi-Nik, A. Bahari, A. Sadeghi-Nik, and E. Mirshafiei. 2016. "Microstructural characterization and mechanical properties of cementitious mortar containing montmorillonite nanoparticles." *J. Mater. Civ. Eng.* 28 (12): 04016155. [https://doi.org/10.1061/\(ASCE\)MT.1943-5533.0001671](https://doi.org/10.1061/(ASCE)MT.1943-5533.0001671).

- Kumar Mehta, P., and P. J. M. Monteiro. 2013. *Concrete: Microstructure, properties and materials*. 4th ed. New York: McGraw Hill.
- Leong, Y. K., P. J. Scales, T. W. Healy, and D. V. Boger. 1995. "Interparticle forces arising from adsorbed poly-electrolytes in colloidal suspensions." *Colloids Surf., A* 95 (3): 43–52. [https://doi.org/10.1016/0927-7757\(94\)03010-W](https://doi.org/10.1016/0927-7757(94)03010-W).
- Manzur, T., S. Iffat, and M. A. Noor. 2015. "Efficiency of sodium polyacrylate to improve durability of concrete under adverse curing condition." *Adv. Mater. Sci. Eng.* 2015 (12): 1–8. <https://doi.org/10.1155/2015/685785>.
- Mathieu, Y., B. Lebeau, and V. Valtchev. 2007. "Control of the morphology and particle size of boehmite nanoparticles synthesized under hydrothermal conditions." *Langmuir* 23 (18): 9435–9442. <https://doi.org/10.1021/la700233q>.
- Mathieu, Y., S. Rigolet, V. Valtchev, and B. Lebeau. 2008. "Investigations of a sodium–polyacrylate-containing system yielding nanosized boehmite particles." *J. Phys. Chem.* 112 (47): 18384–18392. <https://doi.org/10.1021/jp806404e>.
- Moroz, E. M., D. A. Zyuzin, K. I. Shefer, A. S. Ivanova, E. V. Kulko, V. V. Goidin, and V. V. Molchanov. 2006. "Local structure of pseudoboehmites." *React. Kinet. Catal. Lett.* 87 (2): 367–375. <https://doi.org/10.1007/s11144-006-0045-z>.
- Munhoz, A. H., Jr., M. V. Martins, V. Ussui, K. Cruz, A. R. Zandonadi, and L. F. Miranda. 2012. "The influence of ageing in pseudoboehmites synthesis." *Mater. Sci. Forum* 727 (12): 1795–1801. <https://doi.org/10.4028/www.scientific.net/MSF.727-728.1795>.
- Musić, S., D. Dragčević, and S. Popović. 1999. "Hydrothermal crystallization of boehmite from freshly precipitated aluminium hydroxide." *Mater. Lett.* 40 (6): 269–274. [https://doi.org/10.1016/S0167-577X\(99\)00088-9](https://doi.org/10.1016/S0167-577X(99)00088-9).
- Musić, S., D. Dstrok, S. Popović, and N. Vdović. 1998. "Microstructural properties of boehmite formed under hydrothermal conditions." *Mater. Sci. Eng.* 52 (2–3): 145–153. [https://doi.org/10.1016/S0921-5107\(97\)00277-8](https://doi.org/10.1016/S0921-5107(97)00277-8).
- Neville, A. M. 2006. *Neville on concrete: An examination of issues in concrete practice*. Farmington Hills, MI: Booksurge.
- Ng, D. S., S. C. Paul, V. Anggraini, S. Y. Kong, T. S. Qureshi, C. R. Rodriguez, Q. F. Liu, and B. Šavija. 2020. "Influence of SiO₂, TiO₂ and Fe₂O₃ nanoparticles on the properties of fly ash blended cement mortars." *Constr. Build. Mater.* 258 (1): 119627. <https://doi.org/10.1016/j.conbuildmat.2020.119627>.
- Niewiadomski, P. 2015. "Short overview of the effects of nanoparticles on mechanical properties of concrete." *Key Eng. Mater.* 662 (2015): 257–260. <https://doi.org/10.4028/www.scientific.net/KEM.662.257>.
- Ram, S. 2001. "Infrared spectral study of molecular vibrations in amorphous nanocrystalline and AlO(OH)·H₂O bulk crystals." *Infrared Phys. Technol.* 42 (Jan): 547–560. [https://doi.org/10.1016/S1350-4495\(01\)00117-7](https://doi.org/10.1016/S1350-4495(01)00117-7).
- Richerson, D. W. 1992. *Modern ceramic engineering*. New York: Marcel Dekker.
- Silva, G. F., S. Martini, J. C. B. Moraes, and L. K. Teles. 2021. "AC impedance spectroscopy (AC-IS) analysis to characterize the effect of nanomaterials in cement-based mortars." *Constr. Build. Mater.* 269 (Jan): 121260. <https://doi.org/10.1016/j.conbuildmat.2020.121260>.
- Sing, K. S. W., D. H. Everett, R. A. W. Haul, L. Moscou, R. A. Pirotti, J. Rouquérol, and T. Siemieniowska. 1985. "Reporting physisorption data for gas/solid systems with special reference to the determination of surface area and porosity." *Pure Appl. Chem.* 57 (4): 603–619.
- Tam, V. W. Y., M. Soomro, and A. C. Jorge Evangelista. 2018. "A review of recycled aggregate in concrete applications (2000–2017)." *Constr. Build. Mater.* 172 (Mar): 272–292. <https://doi.org/10.1016/j.conbuildmat.2018.03.240>.
- Vishwakarma, V., and D. Ramachandran. 2018. "Green concrete mix using solid waste and nanoparticles as alternatives—A review." *Constr. Build. Mater.* 162 (11): 96–103. <https://doi.org/10.1016/j.conbuildmat.2017.11.174>.
- Xiao, J., N. Han, and Y. Li. 2021. "Review of recent developments in cement composites reinforced with fibers and nanomaterials." *Front. Struct. Civ. Eng.* 15 (21): 1–19. <https://doi.org/10.1007/s11709-021-0723-y>.
- Yeon, J. H. 2021. "Restrained stress development in hardening mortar internally cured with superabsorbent polymers under autogenous and drying conditions." *Polymers* 13 (4): 979. <https://doi.org/10.3390/polym13060979>.